



Bearing fault diagnosis based on optimal Morlet wavelet filter and Teager-Kaiser energy operator

Hocine Bendjama¹

Received: 21 February 2022 / Accepted: 13 July 2022 / Published online: 10 August 2022
© The Author(s), under exclusive licence to The Brazilian Society of Mechanical Sciences and Engineering 2022

Abstract

A defective rolling bearing usually generates repetitive impulses often appears as an amplitude modulated signal, which contains fault feature. To assess the faulty bearings, a proper signal processing method is necessary to extract the fault information from the periodic impulses submerged in heavy background noise and interference vibrations. This paper presents a new Combined Time–Frequency Method (CTFM) based on Morlet Wavelet Filter (MWF), Intrinsic Time-scale Decomposition (ITD), and Teager-Kaiser (TK) energy operator to extract impulsive features for better evaluating bearing operating conditions. The MWF with predefined parameters (center frequency and bandwidth) is used to remove background noise from bearing vibration signal. The filtered signal, which is a multi-component signal, is decomposed into Proper Rotation Components (PRCs) through ITD method, followed by an error analysis to select the most significant PRCs in order to eliminate interference components. Then, the bearing vibration signal is reconstructed from the selected components and its energy is estimated using the TK operator. According to the maximum energy value, the power spectrum of the TK envelope or modulating signal is used for clear visualization of the Bearing Characteristic Frequencies (BCFs) as well as the optimal parameters of the Morlet filter are retained. To test its performance, the proposed CTFM is applied on simulated and experimental bearing signals and discussed by comparing its performance to previous studies. The obtained results demonstrate the effectiveness of the CTFM in identifying BCFs.

Keywords Fault diagnosis · Morlet wavelet · Intrinsic time-scale decomposition · Teager-Kaiser operator · Rolling bearing

1 Introduction

Rotating machinery plays a significant role in various industrial applications. It generally works under severe conditions making the key parts such as gears and bearings subject to faults. Generally, bearing defects may occur on the inner race, the outer race or the ball. During the passage of the rolling element over the defect, an impulse signal containing useful fault information is generated periodically with a time period corresponding to Bearing Characteristic Frequencies (BCFs). These repetitive impulses appear as a very sharp rise that excites the high frequency resonance of the structure, where the bearing is mounted, and quickly decay

due to the internal damping of the system, which enables the vibration signals to present the mechanism of amplitude modulation [1]. The periodic impulses are short in time duration and usually contaminated by noise and other vibration interferences. Therefore, the effective extraction of the fault information from bearing signals becomes a challenging issue.

In recent years, a wide variety of signal processing methods have been proposed and applied to reduce noise components and extract useful information from bearing signals. Moreover, the bearing vibration signal is usually non-stationary, which requires more suitable methods such as wavelet transform [2]. Wavelet transform, introduced by Morlet in 1984, is one of the most powerful signal processing techniques. It is widely used to analyze non-stationary signals due to its good time–frequency localization properties. Morlet wavelet is defined as a cosine function that decays exponentially on both sides, and its function shape is very much like an impulsive feature. Due to its similarity to the bearing impulse signal, it is widely used to detect the

Technical Editor: Jarir Mahfoud.

✉ Hocine Bendjama
h.bendjama@crti.dz

¹ Research Center in Industrial Technologies CRTI,
P.O.Box 64, Cheraga, Algiers, Algeria

periodical impulses that indicate the occurrence of bearing faults.

Morlet wavelet can be viewed as a filtering process that has the ability of separating the different features of the noise and the useful signal. However, the major challenge in this application is the proper optimization of the Morlet Wavelet Filter (MWF) parameters: center frequency and bandwidth, in order to achieve an optimal match with the signal. To select the most favorable pair of parameters, different techniques are developed and proposed to detect the impact signal with good time–frequency resolution. Nikolaou and Antoniadis [3] used an entropy-magnification combined factor to optimize parameters in a way that can analyze the modulation mechanism present in the impulsive response of faulty bearings. He et al. [4] optimized the wavelet filter by differential evolution to obtain the fault characteristic signal. Su et al. [5] proposed a hybrid method that combines optimal MWF and autocorrelation enhancement algorithm to enhance the periodic impulsive features and remove the residual noise, where the center frequency and bandwidth parameters are optimized by genetic algorithm. Jiang et al. [6] designed a denoising method to achieve an optimal match with the impulsive signals, where the modified Shannon wavelet entropy is used to optimize the shape and bandwidth parameter of the Morlet wavelet. Also, the singular value decomposition is performed to select the appropriate transform scale. Zhang et al. [7] filtered the bearing vibrations with an MWF whose bandwidth and center frequency parameters are determined using local mean decomposition and Shannon entropy criterion. Cao et al. [8] optimized the Morlet parameters using a modified algorithm based on the Shannon entropy and then extracted the impact signal through a modified adaptive method.

Actually, even without noise after filtering, the periodical impulses of the bearing are multi-component signals due to vibration interferences. Therefore, the best way is to decompose a multi-component signal into a sum of mono-component signals to extract the useful information from the resulting signals. For this purpose, several decomposition techniques were adopted over the years, including Empirical Mode Decomposition (EMD) [9], Local Mean Decomposition [10], and Intrinsic Time-scale Decomposition (ITD) [11]. The EMD and LMD methods can self-adaptively decompose the nonlinear and non-stationary signal into the sum of several components of intrinsic mode function and product function, respectively. However, some inevitable limitations often appear when using EMD and LMD, such as mode mixing and end effects. On the other hand, the ITD is a self-adaptive approach that has high decomposition efficiency and frequency resolution. The multi-component non-stationary signal is decomposed into a number of Proper Rotation Components (PRCs) and a trend component. The ITD can effectively overcome the limitations of EMD and

LMD. As it only requires linear interpolation and has no need for a sifting process, the ITD method can extract useful features from vibration signals with higher efficiency and shorter computing time than EMD and LMD.

In the last few years, the ITD algorithm has been successfully applied as a powerful tool to analyze the bearing vibration signals [12–14]. The selection of the most valuable PRCs is a very important step in the ITD approach. Although, some researchers consider only the first few rotation components [15]. However, most studies, in this field, applied various selection criteria to discriminate whether the PRC is valuable or not, such as Lempel–Ziv complexity [12], weighted kurtosis [13], Shannon entropy [16], and Laplacian energy-based criterion [14]. In another application, the PRC with an instantaneous frequency fluctuating around the gear meshing frequency or its harmonics is selected as a sensitive mono-component for planetary gearbox fault diagnosis [17].

In fact, the impulsive bearing fault signal can be viewed as an amplitude modulated signal in the natural frequency resonance signal (the carrier) in which the modulating signal (the envelope) includes the frequency components associated with the characteristic frequency of the faulty bearing and harmonics. Therefore, the analysis of the envelope signal is an important task for extracting the BCF from the carrier frequency. In the last decades, the amplitude modulated signal is extracted using the envelope analysis [18] that is based on band-pass filtering of the bearing vibration signal. Unfortunately, the correct selection of the filters' bandwidth is difficult. Recently, the envelope signal can be demodulated using the Teager-Kaiser (TK) energy operator. The TK operator is an effective tool for analyzing nonlinear signals to extract the amplitude modulated signal and then, the fault characteristics. To transform the vibration signal in the TK domain in order to evaluate its energy measurement has been studied by several works [19–22].

This paper aims at transforming the reconstructed vibration signal resulting from the MWF and ITD into the TK domain to optimize the filter parameters to achieve impulse signal extraction for bearing condition monitoring. Firstly, the bandwidth and center frequency ranges of the MWF are defined to obtain the filtered signal. The multi-component resulting signal requires a mono-component decomposition (PRCs) using the ITD approach to eliminate the interfering vibrations. The most representative PRCs that contain rich information are identified to reconstruct the decomposed signal according to a proposed selection criterion based on error measure between the input and each decomposed mode. Then, the mono-component envelope signal, including the BCF, is demodulated in the TK domain to provide us with the optimal Morlet filter and the characteristic frequency using power spectrum. Finally, simulated and real vibration signals, in the cases of inner race fault and outer race fault of rolling bearings, are used to evaluate the

effectiveness of the proposed CTFM over other techniques. The obtained results demonstrate that the proposed method can identify the optimal Morlet filter and also extract the periodic impulses hidden in noises and interferences in the time domain, and detect the dominating components (characteristic frequency and its harmonics) in the frequency domain.

2 Bearing faults

The vibrations produced by damaged bearing elements represent the most common problems in rotating machinery. The different faults occurring in a bearing can be classified according to the defective element as: Inner Race fault (IR), Outer Race fault (OR), and Ball fault (B). When the rolling elements strike a localized fault on the inner or outer race and vice versa, an impulse signal is produced periodically with a time period corresponding to one of the BCFs (Fig. 1).

The BCFs, of a defective bearing, associated with inner race fault (f_{IR}), outer race fault (f_{OR}) and ball fault (f_B) are related to the rotational frequency of the shaft, bearing geometry and defect location. They are calculated as follows:

$$f_{IR} = \frac{Zf_r}{2} \left(1 + \frac{d}{D} \cos(\alpha) \right) \quad (1)$$

$$f_{OR} = \frac{Zf_r}{2} \left(1 - \frac{d}{D} \cos(\alpha) \right) \quad (2)$$

$$f_B = \frac{Df_r}{d} \left(1 - \left(\frac{d}{D} \cos(\alpha) \right)^2 \right) \quad (3)$$

where f_r is the rotational frequency, d the ball diameter, D the pitch diameter, Z the number of balls and α the contact angle. Usually, the impulse signals at these fault frequencies are modulated by the high frequency carrier signal (resonance), which results an exponentially decaying vibration,

as shown in Fig. 1. The key is to find periodic impulses hidden in the measured bearing signals. Therefore, a proper signal processing method, described in the next section, is necessary.

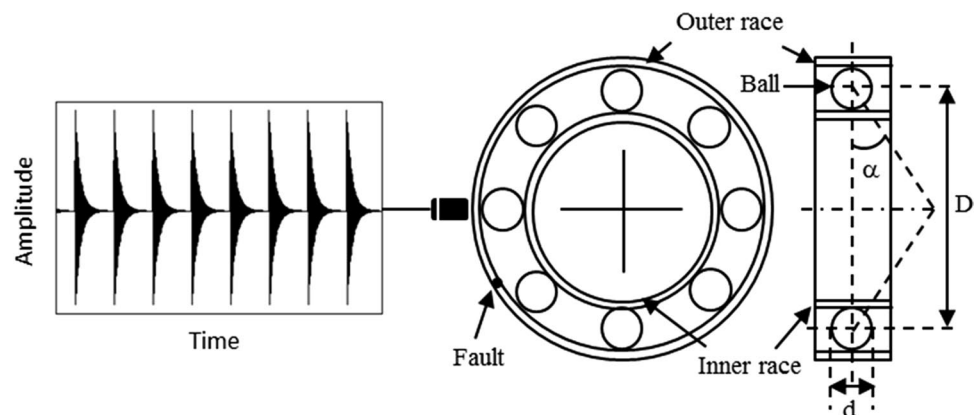
3 Combined time–frequency method (CTFM)

3.1 Principle

With a fault on a particular element of the bearing, a periodically impulsive signal at this element rotational frequency is produced, which may excite the resonances in the bearing. These generated impulses are often appear as an amplitude modulated signal that is usually submerged in background noise and other vibration interferences. Therefore, the extraction of the fault information contained in the periodically impacts has primary importance for the correct operation of the machine. For this purpose, CTFM is proposed.

Figure 2 represents the block diagram of our method. The proposed method can be divided into three major tasks, which are signal filtering, signal decomposition and signal demodulation. To this end, it combines the MWF, ITD, and TK energy operator in order to extract the modulating signal with the optimal center frequency and bandwidth of MWF. After reducing the background noise, the resulting signal is a multi-component signal which requires isolating each component before applying the TK transform. Through ITD, the filtered signal is decomposed into a series of components (PRCs) and the most significant PRCs are selected using a criterion based on the energy of error between the original signal and each decomposed component. Energy values above a threshold line indicate the most representative PRCs, and are thus used in signal reconstruction. Then, the TK operator allows demodulating the reconstructed signal and calculating the energy of the obtained envelope by applying a new proposed indicator. The final result is the optimal MWF

Fig. 1 Bearing geometry and impulse signal



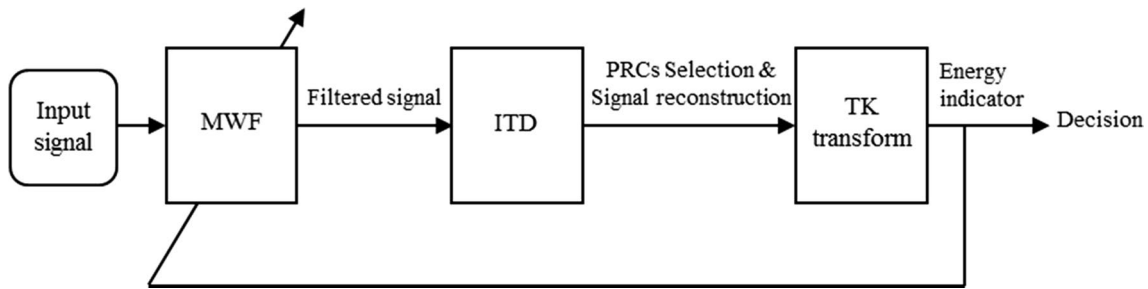


Fig. 2 Principle of the proposed method

and the power spectrum representation of the envelope or demodulated signal having the largest energy value, which contains the BCFs.

3.2 Optimal Morlet wavelet filter

3.2.1 Continuous wavelet transform (CWT)

Wavelet transform is a kind of variable window technology, which uses a time interval to analyze the frequency components of the signal in terms of a wavelet base function, called mother wavelet (Eq. 4).

$$\psi(t) = |a|^{-1/2} \psi\left(\frac{t-b}{a}\right), a, b \in R, a \neq 0 \tag{4}$$

where a and b denote the scale and shift parameters, respectively, while the factor $|a|^{-1/2}$ is used to ensure energy preservation.

The mother wavelet must be compactly supported and satisfied with the admissibility condition as follows

$$\int_{-\infty}^{+\infty} |\hat{\psi}(w)|^2 / |w| dw < +\infty \tag{5}$$

where $\hat{\psi}(w)$ is the Fourier Transform (FT) of $\psi(t)$.

Continuous wavelet transform is particularly suitable for non-stationary measures analysis. It is described as follows: let $x(t)$ be the original signal; the CWT of $x(t)$ is defined as follows:

$$CWT(a, b) = |a|^{-1/2} \int_{-\infty}^{+\infty} x(t) \psi^*\left(\frac{t-b}{a}\right) dt \tag{6}$$

where $\psi^*(t)$ is the conjugate function of the mother wavelet $\psi(t)$. According to the convolution theorem and FT properties, Eq. 6 can be expressed as follows:

$$W_b(a) = \left(1/\sqrt{a}\right) F^{-1}\{X(f)\Psi^*(af)\} \tag{7}$$

where $X(f)$ and $\Psi^*(f)$ represent the FT of $x(t)$ and $\psi^*(t)$, respectively, and F^{-1} denotes the inverse FT.

The CWT analyzes the signal at different scales. It can be regarded, from Eq. 7, as the signal passing through a band-pass filter.

3.2.2 Morlet wavelet filter

The CWT is defined as the inner product between the time signal and the translated and dialed mother wavelet function. Several standard families of wavelet base function can be used such as Haar, Daubechies, Coiflets, Morlet and Symlets [23], where different wavelets serve different purposes. The selection of an appropriate mother wavelet function is an important step and part of wavelet analysis for feature extraction from measured signals [24]. In this work, we use the complex Morlet wavelet according to the Nikolaou and Antoniadis [3], He et al. [4] and Su et al. [5] studies. The reason is the fact that the Morlet function has a similar shape to impulses caused by bearing faults.

The Morlet wavelet is suitable for continuous analysis and its formulation, in the time domain, is defined as a complex exponential function as follows:

$$\psi(t) = c e^{-\sigma^2 t^2} e^{j2\pi f_c t} \tag{8}$$

where c denotes a positive parameter. It is typically chosen according to Eq. 9.

$$c = \sigma / \sqrt{\pi} \tag{9}$$

According to the above choice of c , the FT of the Morlet wavelet is defined as follows:

$$\Psi(f) = \Psi^*(f) = e^{-(\pi^2/\sigma^2)(f-f_c)^2} \tag{10}$$

The Morlet wavelet has the wave shape of a Gaussian window in the frequency domain, where σ and f_c represent the bandwidth and central frequency, respectively. This shape practically covers a frequency band in the range $[f_c - \sigma/2, f_c + \sigma/2]$. Thus we can build a MWF as follows:

$$WT(f_c, \sigma) = F^{-1}\{X(f)\Psi^*(f)\} \tag{11}$$

Figure 3 shows the shapes of Morlet wavelet, in the frequency domain, with different center frequency and a fixed σ value (Fig. 3a), and with different bandwidth filters and a fixed f_c value (Fig. 3b). These shapes comprise rising and decaying parts, where the parameter σ balances their bandwidths. The parameters f_c and σ must be adjusted to identify the impacts hidden in the noisy bearing signal. The selection procedure of their range is discussed in the next section.

3.2.3 MWF construction

In the frequency range, there is a favorable pair of f_c and σ parameters that provide an appropriate time–frequency resolution for the bearing signal. For specific values, the time signal resulting from Eq. 11 is considered to be analytic since the function Ψ is real. The modulus of this analytic result represents the envelope of the band-pass filtered signal (Eq. (12)).

$$c(t) = |\text{WT}(f_c, \sigma)| \tag{12}$$

The envelop analysis aims to separate the low-frequency information of the impulsive signal, the obtained envelope must be characterized to adjust f_c and σ to construct an optimal band-pass filter. The construction procedure will be detailed in Sect. 3.4.1.

In order to adjust the MWF parameters, certain conditions must be achieved. These conditions are formulated, according to He et al. [4] and Su et al. [5], as follows:

- Firstly, the wavelet should satisfy the admissibility condition (Eq. 5) which is equivalent to the following requirement

$$\psi(0) = \int_{-\infty}^{+\infty} \psi(t)dt = 0 \tag{13}$$

As it is widely known, the Morlet wavelet does not satisfy this zero-mean requirement. However, the mean can become infinitely small if the term f_c/σ is sufficiently large. When $f_c/\sigma > 1.3$, there is $\psi(0) < 5 \times 10^{-8}$. Therefore, the admissibility condition can be approximately satisfied, when $\sigma < 1.3/f_c$.

- Then, according to the sampling theorem, the upper cut-off frequency of MWF $f_c + 0.5\sigma$ must satisfy

$$f_c + 0.5\sigma < f_{Nyq} \tag{14}$$

where $f_{Nyq} = f_s/2$ is the Nyquist rate and f_s is the sampling frequency of the signal.

Also, the lower cut-off frequency of MWF $f_c - 0.5\sigma$ should be sufficiently large in order to reduce the interference effects of the shaft harmonics, as follows:

$$f_c - 0.5\sigma \geq Nf_r \tag{15}$$

where f_r is the frequency of rotation of the shaft and N is an integer that should be sufficiently large in order to reduce the interference effects from the shaft harmonics. In this paper, it is typically chosen as 30.

- Finally, the bandwidth of the MWF must also be sufficiently wide to fully extract the impulsive feature. Here, it is chosen as follows:

$$\sigma > 3f_d \tag{16}$$

where f_d is the Ball-Passing Frequency Inner-race (BPFI). It is the biggest one of the BCFs.

So, the optimal f_c and σ of the MWF must meet the above conditions. They are summarized as follows:

Max Energy indicator (E_{n_i})

$$S.t. f_c/\sigma > 1.3 \tag{17}$$

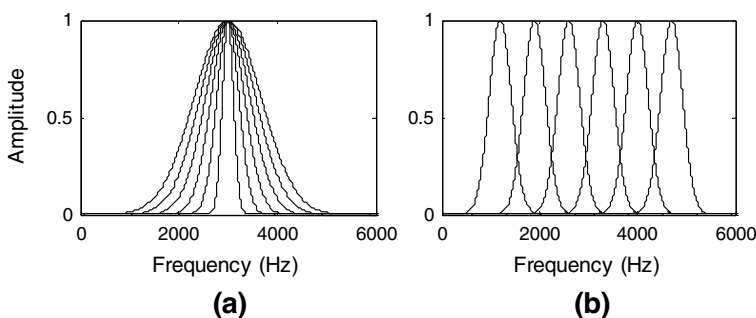
$$f_c + 0.5\sigma < f_{Nyq} \tag{18}$$

$$f_c - 0.5\sigma \geq Nf_r \tag{19}$$

$$\sigma > 3f_d \tag{20}$$

Different bandwidths of the Morlet wavelet filters and several center frequencies can be established, respectively, with $\sigma \in [3f_d, 0.4f_{Nyq}]$ and $f_c \in [0.2f_{Nyq}, 0.8f_{Nyq}]$. The center frequency must coincide with a resonant frequency and the bandwidth should be chosen as large as necessary in order to include characteristic frequencies related to bearing faults. The selection of optimal parameters is based on

Fig. 3 Shapes of Morlet filter with: **a** Different bandwidths and **b** Different center frequencies



an energy indicator of the TK envelope. Before detailing the selection criteria, the multi-component filtered signal must be decomposed into mono-component signals using the ITD to select the significant components from other vibration components.

3.3 Intrinsic time-scale decomposition (ITD)

The ITD, proposed by Frei et al. [11], is a self-adaptive decomposition method especially suitable for nonlinear and non-stationary signals analysis. The ITD can decompose an input signal into a series of oscillating modes (or PRCs), and a monotonic trend signal, called baseline. The latter is defined as a linearly transformed contraction of the input signal. In the decomposed PRCs, all local maxima and all local minima are strictly positive and negative, respectively. The decomposition procedure is repeated several times, using the baseline signal as a new input, until the baseline becomes a monotonic function or a constant value. To obtain a PRC from an input signal, the procedure introduced as follows:

For a signal $x(t)$, the operator L is defined as an operator extracting a baseline signal from the signal $x(t)$ and the residual signal H is a proper rotation. More specifically, $x(t)$ can be decomposed as follows:

$$x(t) = Lx(t) + (1 - L)x(t) = L(t) + H(t) \tag{21}$$

where $L(t) = Lx(t)$ is the baseline signal and $H(t) = (1-L)x(t)$ denotes the proper rotation component. Let $\{\tau_k, k = 1, 2, \dots\}$ be the local extrema of $x(t)$, and $\tau_0 = 0$. Suppose that $L(t)$ and $H(t)$ are given over the interval $[0, \tau_k]$, and $x(t)$ is available on $[\tau_k, \tau_{k+2}]$. To simplify notation, let x_k and L_k denote $x(\tau_k)$ and $L(\tau_k)$, respectively. The baseline extracting operator, L , is defined as a piecewise linear function on the interval $[\tau_k, \tau_{k+1}]$ between adjacent extrema x_k and x_{k+1} as follows:

$$Lx(t) = L(t) = L_k + \frac{L_{k+1} - L_k}{L_{k+2} - L_k} (x(t) - x_k), \quad t \in [\tau_k, \tau_{k+1}], \tag{22}$$

where

$$L_{k+1} = \alpha \left[x_k + \frac{\tau_{k+1} - \tau_k}{\tau_{k+2} - \tau_k} (x_{k+2} - x_k) \right] + (1 - \alpha)x_{k+1}, \tag{23}$$

and $0 < \alpha < 1$, usually α is around 0.5.

The proper rotation component, H , is expressed as follows:

$$H(t) = Hx(t) = x(t) - Lx(t) = x(t) - L(t) \tag{24}$$

Given the above definitions, the ITD algorithm can be described as follows:

- Step1: Find the local extrema of the input signal $x(t)$, denoted by x_k , and the corresponding occurrence time instant τ_k ,
- Step2: Define the baseline signal, L , of x_k according to Eqs. 22 and 23,
- Step3: Extract the residual signal as PRC, H , according to Eq. 24,
- Step4: Treat L as the input signal, and repeat the above steps, until the baseline becomes a monotonic function or a constant value.

Finally, the signal $x(t)$ is decomposed into a series of PRCs and a trend signal, as follows:

$$x(t) = \sum_{i=1}^p H_i(t) + L_p(t) \tag{25}$$

where p is the number of the decomposed PRCs.

The visual selection of the best oscillatory modes among all the obtained PRCs is often wrong. Therefore, the selection of the most significant modes is an important task that is studied in several works as shown in Sect. 1.

3.3.1 Identifying significant PRCs

In this section, we propose to calculate the error vector between the original signal and its decomposed PRCs in order to find the best modes which must be as close as possible to the input signal. It can be calculated according to the following equation

$$e_i(t) = x(t) - H_i(t) \tag{26}$$

where e_i is the i^{th} residual vector. For more clarity on this selection criterion, we have computed the energy of error (e_i) that represents a very reasonable criterion for selecting the significant PRCs. Logically, its small values, after scaling, determine the closest PRCs to the original signal. Thus, the problem is to locate the valuable PRCs where the energy is minimal. To overcome this problem, a thresholding approach called “universal threshold” can be applied, which is inspired from the field of signal denoising. The universal threshold, proposed by Donoho and Johnston [25], is the most used threshold value in the literature, where it can be measured according to the following equation

$$T = v\sqrt{2\ln p} \tag{27}$$

where v and p denote the variance and the number of decomposition modes, respectively.

This thresholding approach is based on estimating the statistical properties of the decomposed PRCs, such as the variance of normalized error values and the total number of decompositions. The calculated threshold value allows

us to choose the confidence limit. Any energy value below this confidence limit is considered to have a normal variance of statistical data and it represents the best PRCs. Due to the high level of variance for all energies that are above the confidence limit, the corresponding PRCs are therefore eliminated completely. After that, we perform signal reconstruction by adding the selected PRCs.

The reconstructed impulsive signal is transformed in the TK domain in order to extract the envelope from the modulated signal and thus obtain the optimized parameters of MWF according to an appropriate energy indicator.

3.4 Teager-Kaiser energy operator

The TK operator is a nonlinear operator which was first proposed by Teager for use in speech processing, and introduced by Kaiser, in 1990, to track and analyze the signal energy [26]. It has a good adaptability to the instantaneous changes in signals and it is suitable for detecting impact characteristics in a modulated signal such as gear or bearing. For any continuous time signal $x(t)$, the energy operator φ , in continuous form, is defined as follows:

$$\varphi_c[x(t)] = [\dot{x}(t)]^2 - x(t)\ddot{x}(t) \quad (28)$$

where $\dot{x}(t) = dx/dt$ and $\ddot{x}(t) = d\dot{x}/dt$. A discrete form of the TK operator, noted φ_d , is given as follows:

$$\varphi_d[x(n)] = x^2(n) - x(n+1)x(n-1) \quad (29)$$

The TK operator is a tracking operator that provides an excellent time resolution. It is very easy to implement efficiently because it requires only three consecutive samples of the measured signal. Its direct application over the bearing vibration signal can perform a more effective estimation of the instantaneous change in amplitude and frequency of the signal.

When a fault occurs in a bearing, a variation in energy appears in the time signal. For this purpose, an appropriate indicator based on a product of energies is proposed as a principal criterion to optimize the parameters of MWF and extract the modulating signal that contains fault features. The formulations and motivations of this indicator are defined in the following subsection.

3.4.1 Parameters optimization

Generally, the vibration signal acquired from a defective bearing is represented as periodic impulses in the time domain and its energy increases around the resonance. By transforming the signal into the TK domain, the Energy distribution (Ed), established by Parseval's theorem, can be computed to extract the feature of the bearing fault signals.

The Parseval's theorem refers to the result where the sum of square of a function is equal to the sum of the square of its transform. In the TK domain, the Parseval's theorem can be defined as the energy of a function in the time domain is equal to the energy of its transform as follows:

$$Ed = \|\varphi_i\|^2/N \quad (30)$$

where φ_i is the i^{th} measurement, N is the number of samples or data points and $\|\ \|\$ denotes the norm operator.

On the other hand, the impulses generated by bearing faults can also be detected using the Energy factor (Ef). Ef is calculated by taking the kurtosis of the TK signal. Therefore, it shows high values as a factor of impulsiveness [18]. It is expressed as follows:

$$Ef = \frac{N \sum_{i=1}^N (\varphi_i - \bar{\varphi})^4}{\left(\sum_{i=1}^N (\varphi_i - \bar{\varphi})^2 \right)^2} \quad (31)$$

where $\bar{\varphi}$ is the average of the TK signal.

The proposed indicator ($En = Ed \times Ef$) is calculated for all resulting TK signals and the corresponding parameters of WMF with the high value of En are selected as the optimal parameters.

In summary, we must first define the bandwidth and central frequency ranges with initial steps. We fix σ and scan all the center frequencies to determine the Morlet wavelet filters and then we calculate the filtered signals for all values of σ . After filtering, the signal must be decomposed into mono-component signals. Through the ITD, the signal is decomposed into several PRCs in which the most significant components are selected using the error energy between the filtered signal and the decomposed modes. We then compute the TK signal or envelope for each pair of parameters (σ, f_c) and its energy value (En). The obtained results are memorized. By comparing the different computed values, we obtain the optimal parameters which correspond to the maximum value of En . Finally, we calculate the power spectrum of the corresponding TK envelope in order to diagnose the bearing conditions. The CTFM algorithm can be summarized in the following section.

3.5 Algorithm CTFM

Input: bearing vibration signal

1. Define the initial ranges of bandwidth $\sigma \in [\sigma_1, \sigma_2]$ and central frequency $f_c \in [f_{c1}, f_{c2}]$, and also choose the initial steps of bandwidth (i) and central frequency (j),
2. Given an initial value of σ that represents the lower bound of the bandwidth range ($\sigma = \sigma_1$) and increase f_c

from f_{c1} to f_{c2} with the step of j ; the MWF is computed according to Eq. (11), the filtered signal is decomposed according to Eqs. (21) and (24), the best PRCs can be obtained from the error energy criterion to allow a perfect reconstruction of the impulsive signal, and then the TK envelope and its energy are obtained from Eqs. (29)-(31),

3. Compute repeatedly as the above step (2) for the whole values of σ , it results in a series of TK signals,
4. Calculate energy values En ,
5. Check maximum energy value and save the corresponding pair of parameters (σ, f_c) which are the optimal bandwidth parameter and the optimal central frequency,
6. From the selected optimal parameters, we compute the power spectrum of the TK envelope to identify the bearing characteristic frequencies.

Output: σ, f_c and BCFs,

4 Numerical simulation and experimental validation

4.1 Simulation study

In this section, we are going to test the algorithm presented in the previous section on a simulated impulse response of a pulse train. The impulse response could be used to model the modulated signal of a faulty bearing by two harmonic frequencies with an exponential decay and is formulated as follows:

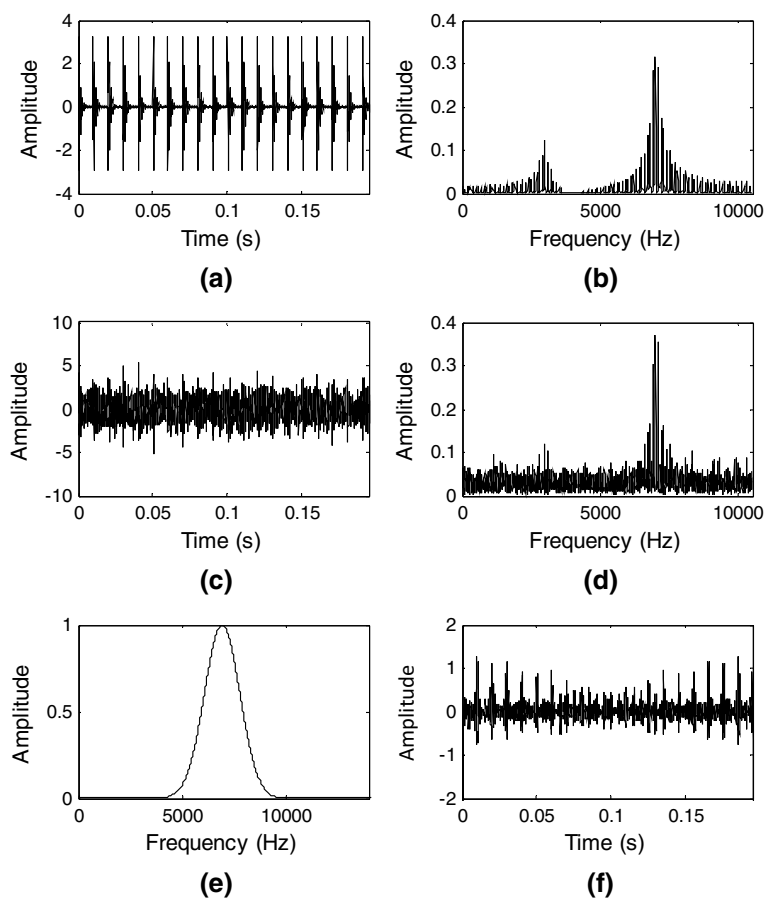
$$x(t) = e^{-\alpha t'} (\sin(2\pi f_1 t) + 1.2 \times \sin(2\pi f_2 t)) \quad (32)$$

with

$$t' = \text{mod}(t, 1/f_d) \quad (33)$$

where α is the exponential decay frequency, f_1 and f_2 are the resonance frequencies, f_d is the defect frequency or modulation frequency.

Fig. 4 **a** Simulated signal without noise and **b** Its spectrum, **c** Signal with noise and **d** Its spectrum, **e** Optimal Morlet filter, **f** Filtered signal



The generated vibration signal, based on Eq. 32, and its frequency spectrum are shown in Fig. 4a and b, respectively. As illustrated in Fig. 4b, the dominant frequency components of 3000 and 7000 Hz are corresponding to two resonance frequencies. Figure 4c and d show the time domain and the frequency spectrum of the simulated signal with a Gaussian noise. Obviously, the periodic impulses shown in Fig. 4c cannot be clearly seen in the time domain compared with Fig. 4a. Note that, the identification of the periodic impacts is a major characteristic of the proposed method. For this purpose, the Morlet wavelet is applied to filter the original vibration signal with various values of σ and f_c within ranges $[3f_d, 0.4f_{Nyq}]$ and $[0.2f_{Nyq}, 0.8f_{Nyq}]$, respectively. At the same time, all filtered signals are decomposed by ITD and the dominant PRCs are selected using the error energy criterion with a confidence limit. The latter is plotted in all figures by a red dot-dashed line. The PRCs with energy values below the threshold line are selected as the dominant PRCs and are then added to reconstruct the input signal. Finally, the reconstructed signal is demodulated by the TK operator in order to estimate the optimal parameters

of MWF and extract the periodic impulses from the bearing vibration signal.

Figure 4f shows the filtered signal using the optimal MWF of Fig. 4e with $\sigma=3783$ Hz and $f_c=6942$ Hz. These values are optimized by computing the energy indicator (En) of the envelope signal, as shown in Fig. 5. According to the maximum value of En , the optimal Morlet filter is selected with a wide bandwidth and a central frequency which is very close to the second resonance frequency of the simulated signal chosen as 7000 Hz. The five decomposed PRCs and the corresponding errors between each PRC and the original signal are plotted in Fig. 6a and b, respectively. By calculating the energy of each error, Fig. 7a shows that the original signal is reconstructed from the first PRC. The TK envelope of the reconstructed signal of Fig. 7b is then extracted and its power spectrum is illustrated in Fig. 8. Many frequency components are present; at the modulation frequency (100 Hz) and its harmonics.

Fig. 5 Optimal parameters of Morlet filter

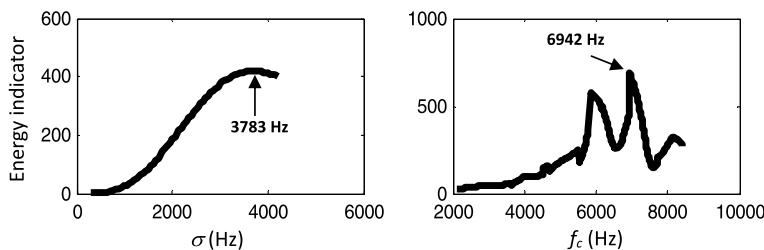


Fig. 6 a PRCs, b Error between each PRC and original signal

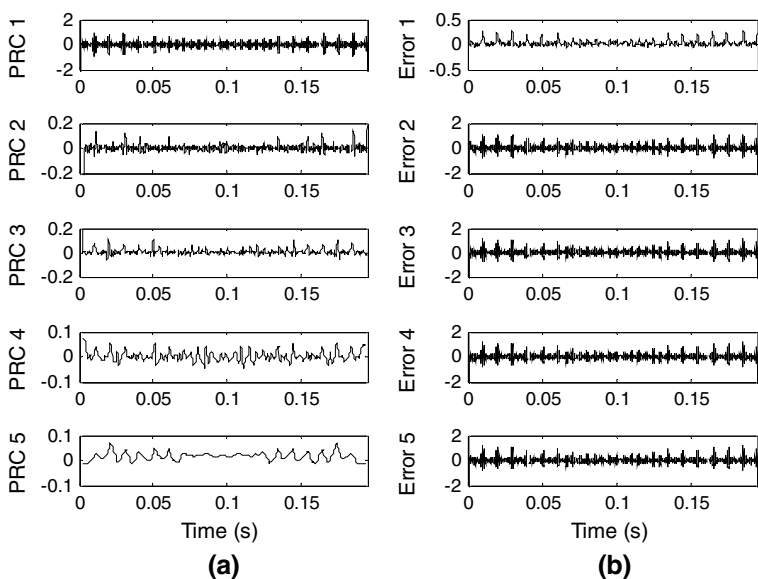


Fig. 7 a Energy of error, b Reconstructed signal

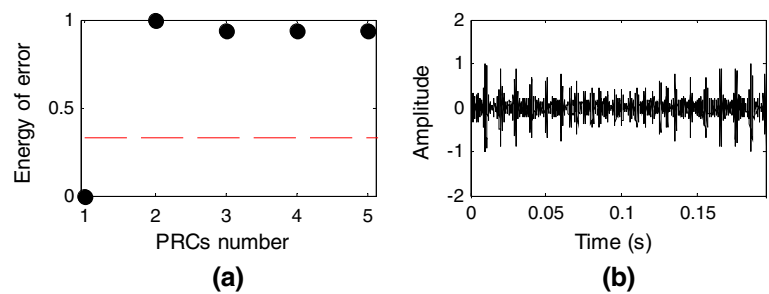


Fig. 8 Envelope power spectrum of the reconstructed signal

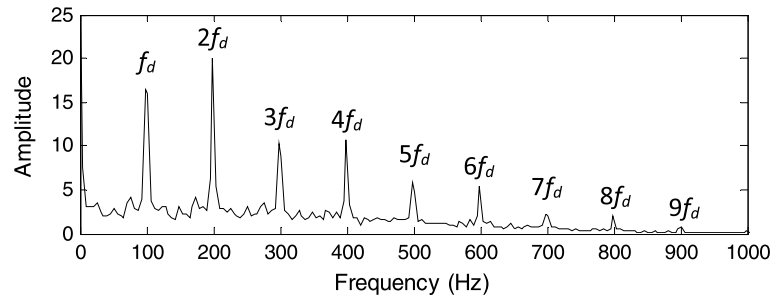
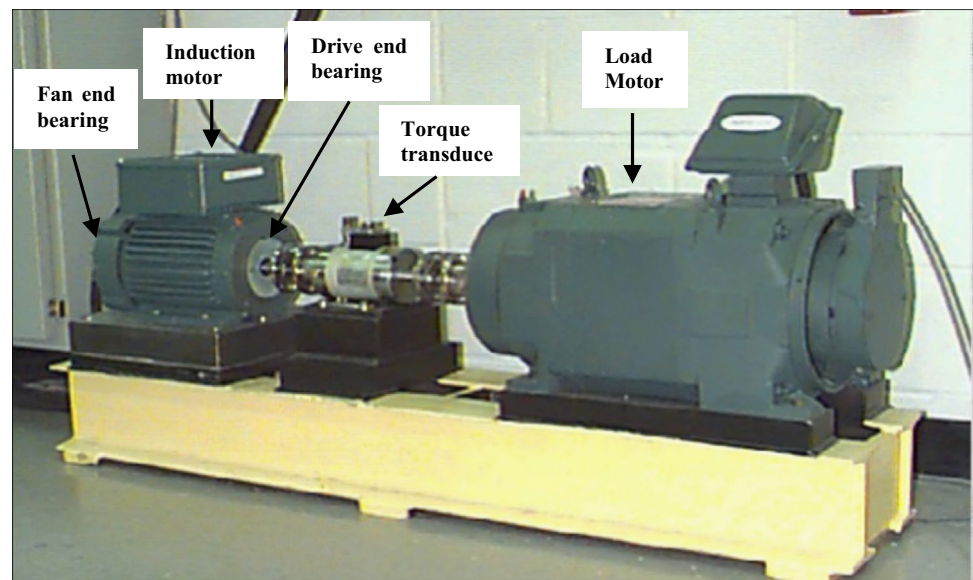


Fig. 9 Bearing test rig



4.2 Experimental test rig

The measurement of vibration applied to condition monitoring and fault diagnosis requires different types and levels of equipment and techniques. These depend on the investment and available expertise.

The experimental measurements presented in this paper are entirely based on the vibration data obtained from the Case Western Reserve University Bearing Data Centre [27]. As shown in Fig. 9, the motor is connected to a dynamometer and torque sensor by a self-aligning coupling.

The vibration signals were collected from an accelerometer mounted on the motor housing at the drive end of the motor. The data were obtained from the experimental system under the four different operating conditions: (1) Normal condition (NR); (2) with inner race fault; (3) with outer race fault and (4) with ball fault. The data is sampled at a rate of 12 kHz and the duration of each vibration signal was 10 s. More details about the experimental setup were reported in [27].

The bearings used in this study are deep groove ball bearings manufactured by SKF. The specifications of the bearing are: ball diameter = 7.94 mm; pitch diameter = 39.04 mm;

Table 1 Bearing model and BCFs in Hz

Bearing model	BCFs (\times rotational speed (rpm))		
	f_{IR}	f_{OR}	f_B
SKF 6205-2RS JEM	0.0903	0.0597	0.0786

Table 2 BCFs of inner race and outer race

Load (hp)	Rotation speed (rpm)	Rotation speed (Hz)	f_{IR} (Hz)	f_{OR} (Hz)
0	1797	29.95	162.27	107.28
1	1772	29.53	160	105.78
2	1750	29.16	158	104.47
3	1730	28.83	156.22	103.28

number of balls = 9; and contact angle = 0. Faults were introduced to the test bearings using electro-discharge machining method with different diameters: 0.018, 0.036, and 0.053 mm. The motor speeds during the experimental tests are: 1797, 1772, 1750 and 1730 rpm. Each bearing was

tested under four different loads: 0, 1, 2, and 3 horsepower (hp). Load is applied using a dynamometer.

The characteristic frequencies of bearing faults can be calculated from the geometry of the bearing and the rotational speed (Eqs. (1)-(3)). The bearing model and BCFs are listed in Table 1.

In this paper, vibration signals collected under four different loads and four different rotation speeds are used for investigations. They are acquired using accelerometers attached to the housing with magnetic bases, including the faults on the inner race and the outer race. The defect sizes are 0.018 mm and 0.053 mm for both inner race and outer race. According to Table 1, the characteristic frequencies of the inner race fault and the outer race fault are computed and listed in Table 2. Each signal has a large number of samples. To improve computing time, we must choose a number of samples that covers a sufficient number of complete rotations. In this study, the motor speed is ranging from 1730 to 1797 rpm, so the selection of a number of 4096 samples allows obtaining nearly 12 complete rotations, which is sufficient for analysis without losing information on the system.

The vibration signals collected at 1797, 1772, 1750 and 1730 rpm from the normal bearing and the defective bearing

Fig. 10 Vibration signals in time domain of normal bearing

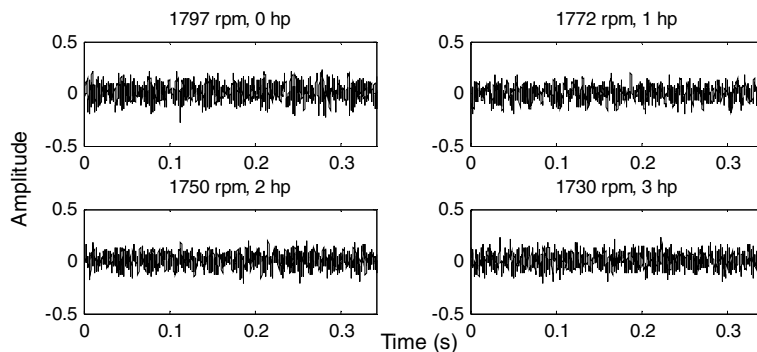


Fig. 11 Vibration signals in time domain of bearing with inner race fault

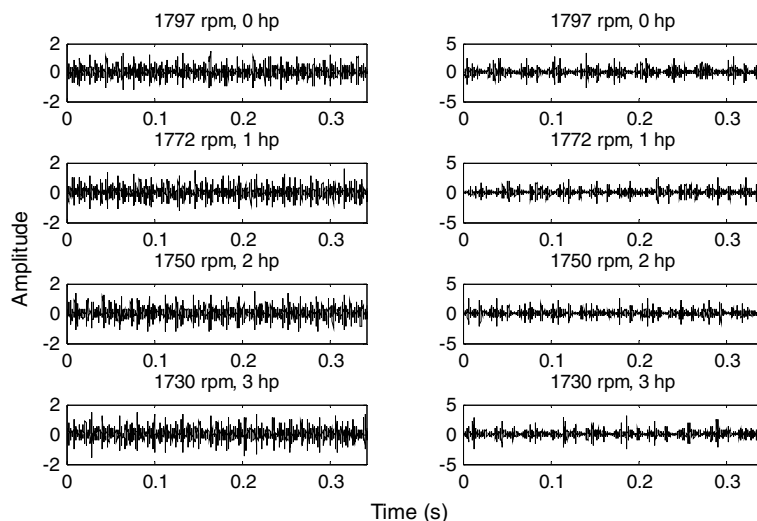


Fig. 12 Vibration signals in time domain of bearing with outer race fault

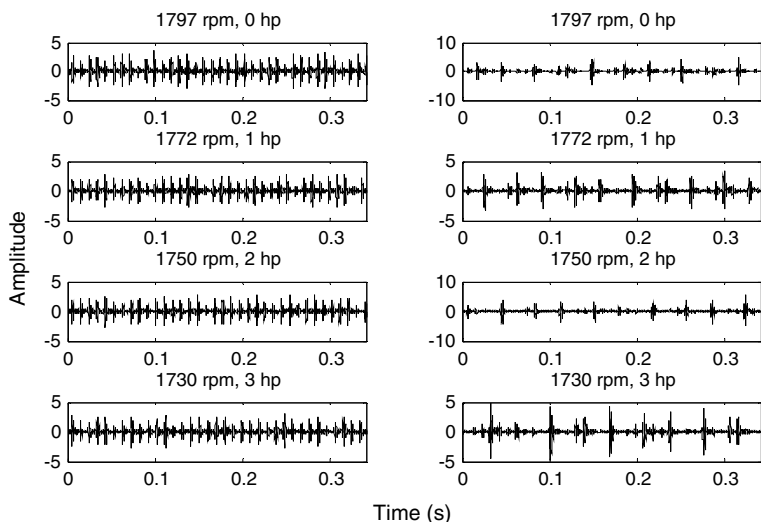
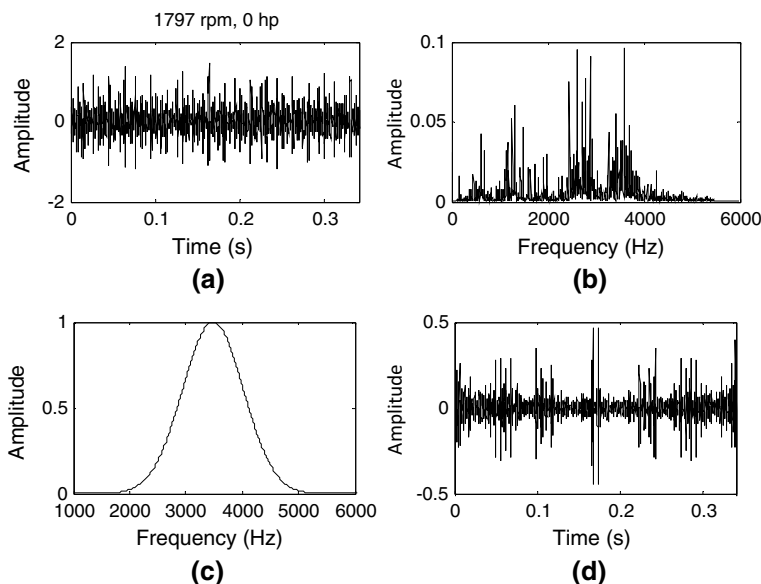


Fig. 13 **a** Vibration signal of bearing with fault diameter of 0.018 mm on the inner race, **b** Spectrum of (a), **c** spectrum of the optimal Morlet filter with $f_c = 3483$ Hz and $\sigma = 2397$ Hz, **d** Filtered signal



with inner race fault and outer race fault are plotted, respectively, in Figs. 10, 11 and 12. From these figures, the impulse responses cannot be directly identified except in the case of outer race fault where they are observed with background noise.

Generally, the experimentally measured signals are marred by noise. This noise produces several frequency components, on the frequency spectrum, which can lead to erroneous conclusions in the interpretation of the results (Figs. 13b, 14b, 15b, 16b, 17b, 18b, 19b and 20b).

The measured signals are processed by the proposed technique to extract the periodic impulses and therefore the fault information. First, the associated noise has been reduced by passing signals through Morlet filters with σ and f_c values defined within reasonable parameter ranges

selected previously. The resulting signals show periodic impulses, but certainly there is no indication of the optimal filter among them. For this purpose, the ITD is combined with the TK in order to estimate the optimal parameters of MWF. Due to the huge amount of results, we have decided to present only some of them, precisely those obtained with the optimal filters. Figures Figs. 13c, 14c, 15c, 16c, 17c, 18c, 19c and 20c and Figs. 13d, 14d, 15d, 16d, 17d, 18d, 19d and 20d represent respectively some results of MWFs with optimized parameters and the corresponding filtered signals. The filtered signals obtained with the optimal filter clearly show the periodic impulses and obviously some noise can be seen in the figures.

After filtering, the obtained impulses of the bearing are multi-component signals which require decomposition into

Fig. 14 **a** Vibration signal of bearing with fault diameter of 0.018 mm on the inner race, **b** Spectrum of (a), **c** Spectrum of the optimal Morlet filter with $f_c = 3438$ Hz and $\sigma = 2400$ Hz, **d** Filtered signal

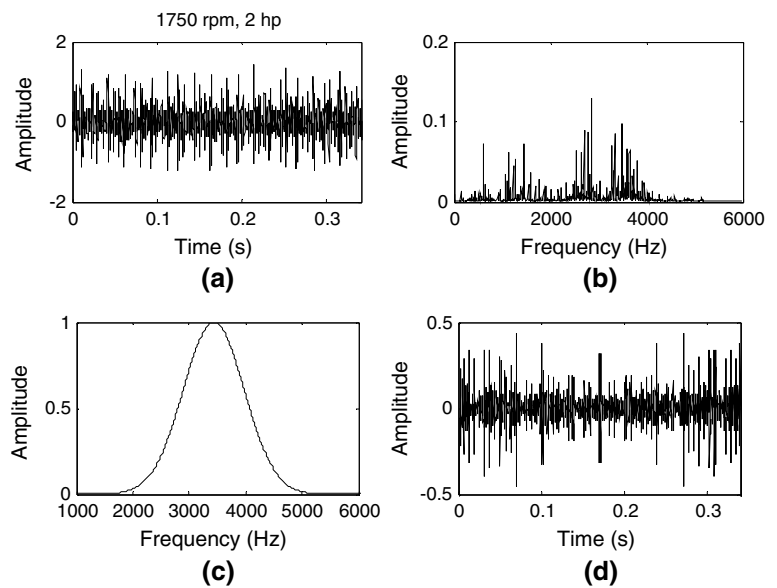
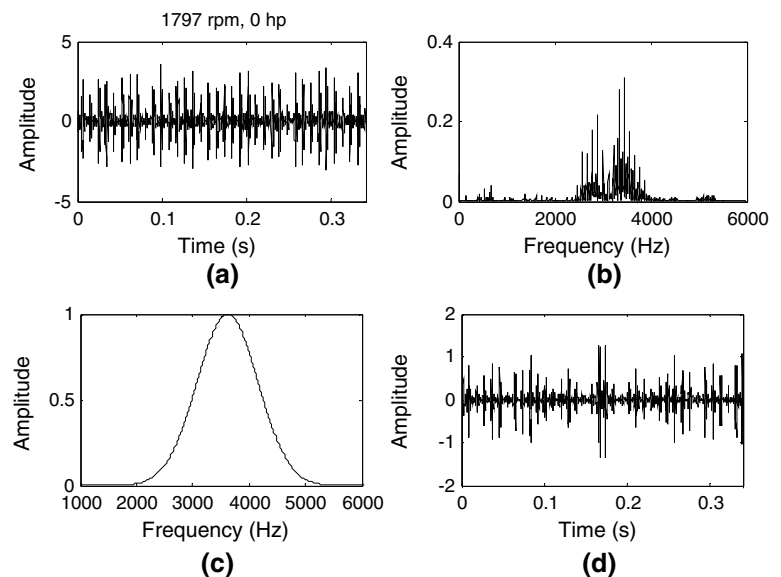


Fig. 15 **a** Vibration signal of bearing with fault diameter of 0.018 mm on the outer race, **b** Spectrum of (a), **c** Spectrum of the optimal Morlet filter with $f_c = 3619$ Hz and $\sigma = 2396$ Hz, **d** Filtered signal



mono-component signals to eliminate vibration interferences. Using the ITD process, a set of mono-components (PRCs) for each filtered signal is generated. For example, Figs. 21a, 22a and 23a and Figs. 21b, 22b, 23b illustrate, respectively, the PRCs and their corresponding errors, for bearing signals measured at 1797 and 1750 rpm with fault diameter of 0.018 mm on the inner race and the outer race.

Some PRCs may contain more information about the condition of the bearing than others. To select the most significant PRCs, the energy of the error between the original signal and each oscillatory mode (PRC) is proposed here as a selection criterion. The computed energy values and the different threshold lines are shown in Figs. 24a, 25a, 26a, 27a, 28a, 29a, 30a and 31a. The selection is performed

by identifying the PRCs that have energy values below the threshold line. In most studied cases, the first PRC has the minimum energy value, so these modes are selected as significant PRCs for signal reconstruction.

The reconstruction signals from the selected modes are displayed in Figs. 24b, 25b, 26b, 27b, 28b, 29b, 30b and 31b. Compared with the input signal (filtered signal), it can be seen clearly that the impulses of bearings appear periodically with time periods.

After that, the TK of each reconstructed signal, in the defined ranges of bandwidth and center frequency, is used to adjust both σ and f_c parameters to obtain an appropriate time–frequency resolution. According to the proposed indicator (En), we can obtain the optimal parameters from the

Fig. 16 **a** Vibration signal of bearing with fault diameter of 0.018 mm on the outer race, **b** Spectrum of (a), **c** Spectrum of the optimal Morlet filter with $f_c = 3558$ Hz and $\sigma = 2396$ Hz, **d** Filtered signal

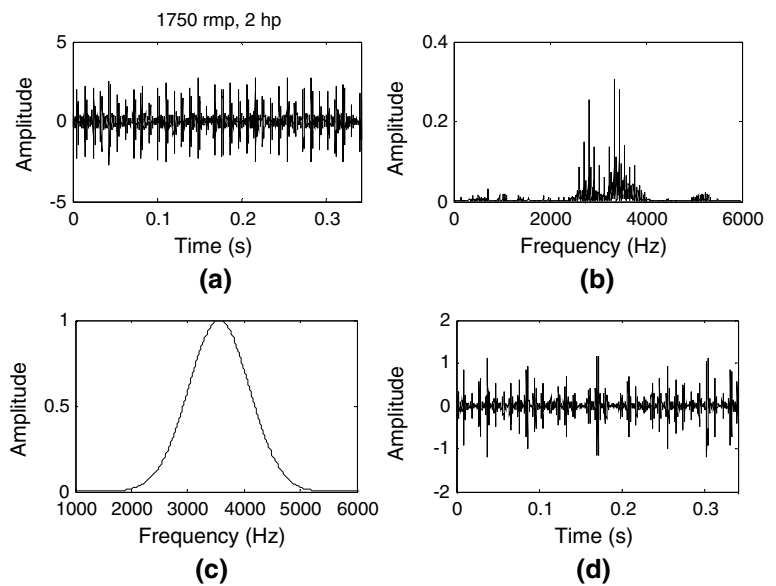
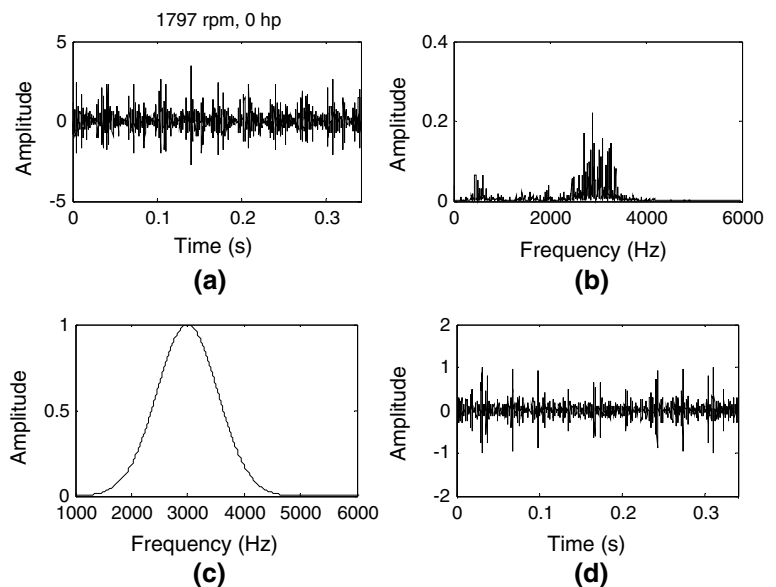


Fig. 17 **a** Vibration signal of bearing with fault diameter of 0.053 mm on the inner race, **b** Spectrum of (a), **c** Spectrum of the optimal Morlet filter with $f_c = 2996$ Hz and $\sigma = 2400$ Hz, **d** Filtered signal



calculated energy values. The σ and f_c corresponding to the maximum value are the optimal bandwidth and the optimal center frequency, respectively. They are listed in Table 3 for the bearing with inner race fault, and in Table 4 for the bearing with outer race fault. We found that the bandwidth frequency is wide and the center frequency is close to the resonance frequency.

Finally, the last step is presented for fault identification by applying the spectral analysis to evaluate the impulsive signal in the frequency domain by using the optimal MWF. Figures 32, 33, 34 and 35 represent spectra of vibration signals acquired from the different conditions of the bearing at four rotating speeds, with and without load. From these figures, many frequency components are clearly found at rotation

frequencies (f_r) and their multiples ($2f_r, \dots$). The BCFs of the inner race and outer race could be also found at the calculated values of f_{IR} and f_{OR} for each condition (Table 2), and their harmonics ($2f_{IR}, 3f_{IR}, \dots$ and $2f_{OR}, 3f_{OR}, \dots$) are present in the frequency spectra. It is also noted in Figs. 32 and 33, only for bearing with IR fault, the presence of sidebands (spaced at f_r) around the BCFs and their harmonics.

The vibration signals acquired from normal bearing at four shaft speeds with four loads are used for evaluating the performance of the proposed CTFM. After signal filtering, signal decomposition and signal demodulation using respectively MWF, ITD and TK operator, the optimal Morlet filter is selected with the large value of σ in the bandwidth range and the small value of f_c in its range, except for the bearing

Fig. 18 **a** Vibration signal of bearing with fault diameter of 0.053 mm on the inner race, **b** Spectrum of (a), **c** Spectrum of the optimal Morlet filter with $f_c = 2949$ Hz and $\sigma = 2400$ Hz, **d** Filtered signal

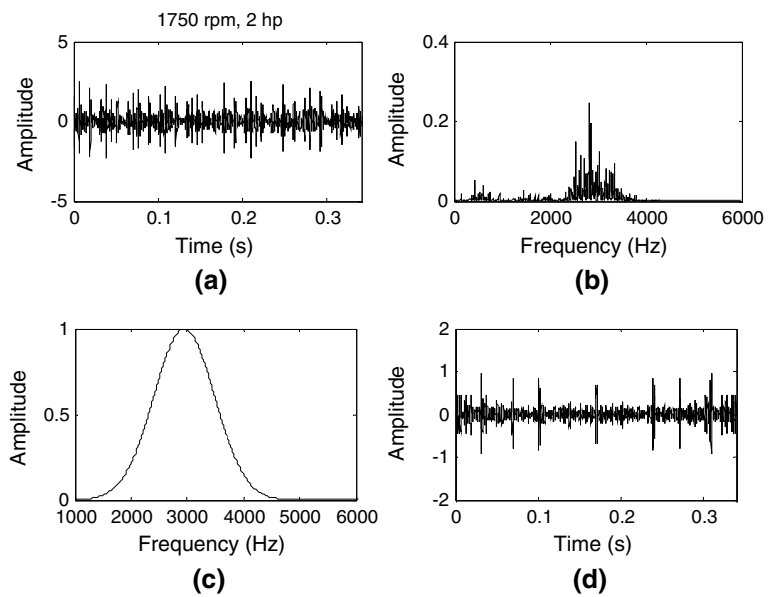
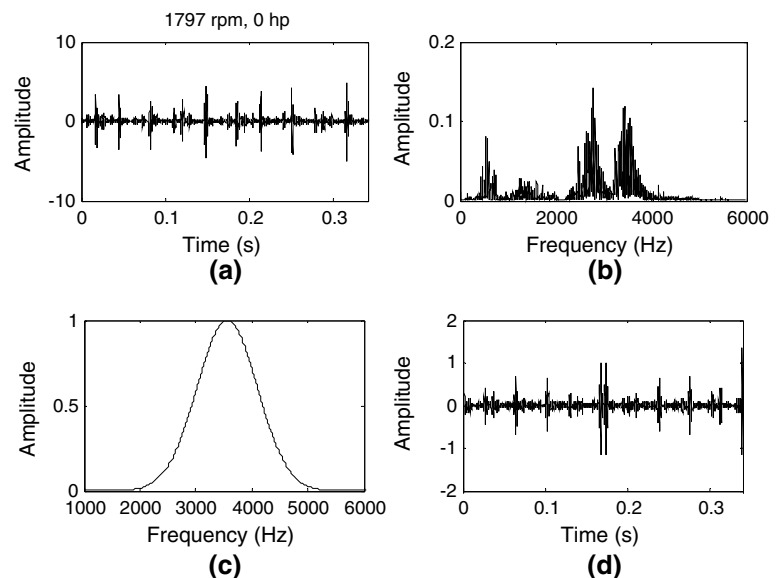


Fig. 19 **a** Vibration signal of bearing with fault diameter of 0.053 mm on the outer race, **b** Spectrum of (a), **c** Spectrum of the optimal Morlet filter with $f_c = 3562$ Hz and $\sigma = 2396$ Hz, **d** Filtered signal



signal measured at 1730 rpm, where the central frequency is 1206 Hz. Figure 36 shows envelope spectra of TK signals of the four considered cases. It can be seen that the rotation frequencies of the shaft (f_r) and their multiples ($2f_r$) can be found in the frequency spectra. As discussed above, the shaft rotational frequency can be clearly detected from a bearing running in normal and faulty conditions by using our method.

On the other hand, the obtained results prove that the proposed method could be effectively applied to extract useful features from bearing vibration signals using optimal filters with wide bandwidths and center frequencies close to

resonance frequencies compared to previous studies reported in [4, 28–30]. Where these studies were carried out with vibration signals collected under different bearing conditions than those used in our study. However, the results listed in Table 5 show that our approach provides a significant improvement over previous results obtained on the same data [5]. Only the vibration signals acquired at 1772 rpm (1 hp) from normal bearing and faulty bearing with defect size of 0.018 mm on inner race and outer race are used for comparison, but these signals summarize the results of other vibration signals obtained from the three studied conditions (NR, IR, and OR) of the bearing operating under various rotational speeds and loads.

Fig. 20 **a** Vibration signal of bearing with fault diameter of 0.053 mm on the outer race, **b** Spectrum of (a), **c** Spectrum of the optimal Morlet filter with $f_c=3535$ Hz and $\sigma=2397$ Hz, **d** Filtered signal

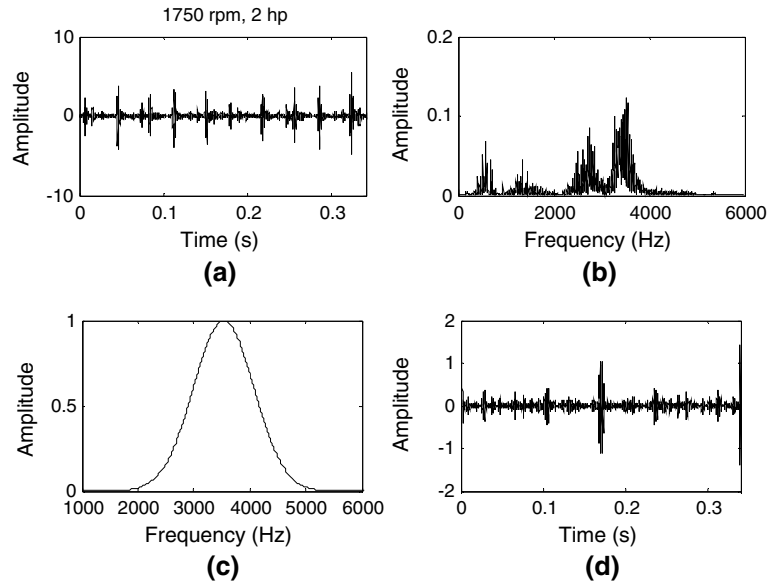


Fig. 21 **a** PRCs, **b** Error between each PRC and original signal of bearing with fault diameter of 0.018 mm on the inner race measured at 1797 rpm and 0 hp

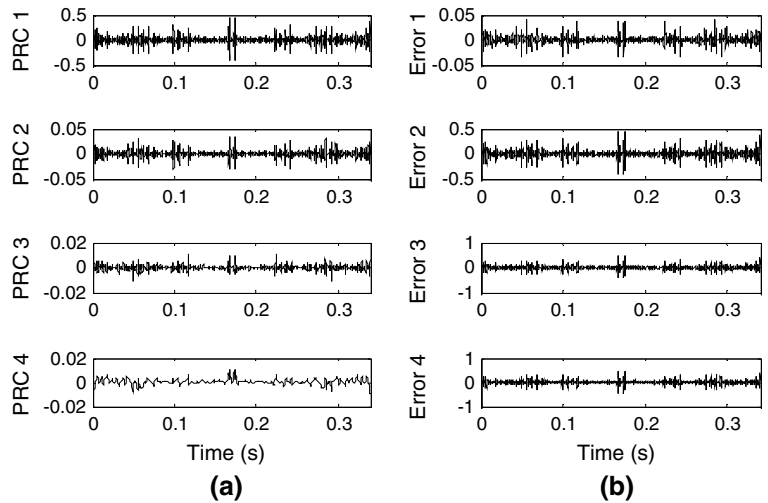


Fig. 22 **a** PRCs, **b** Error between each PRC and original signal of bearing with fault diameter of 0.018 mm on the inner race measured at 1750 rpm and 2 hp

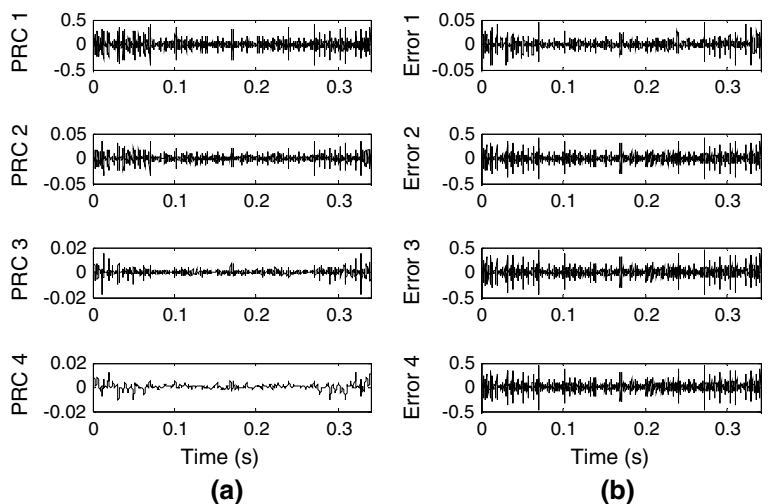


Fig. 23 **a** PRCs, **b** Error between each PRC and original signal of bearing with fault diameter of 0.018 mm on the outer race measured at 1797 and 0 hp

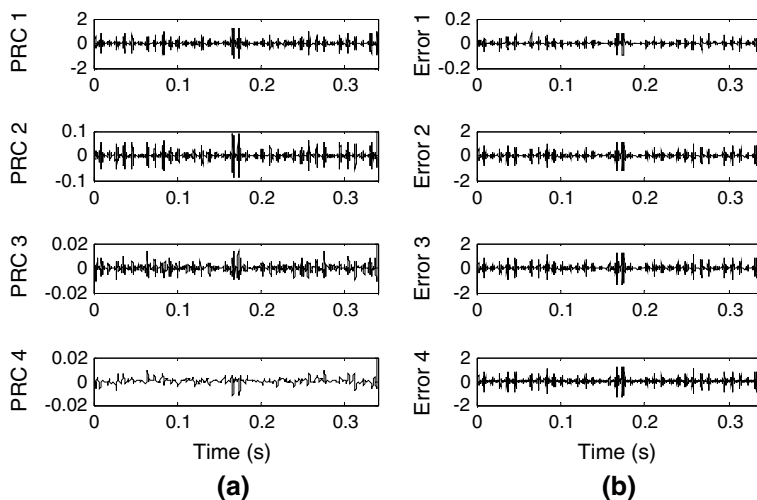


Fig. 24 **a** Energy of error, **b** Reconstructed signal of bearing with fault diameter of 0.018 mm on the inner race measured at 1797 rpm and 0 hp

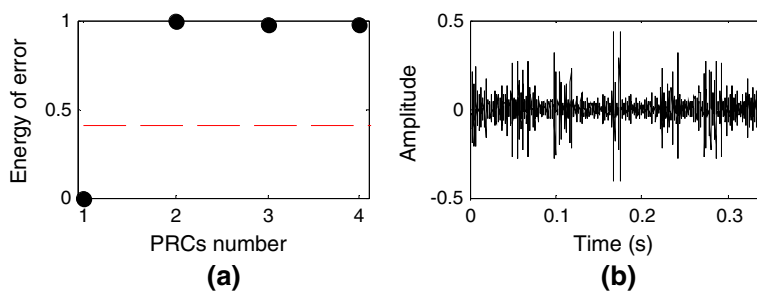


Fig. 25 **a** Energy of error, **b** Reconstructed signal of bearing with fault diameter of 0.018 mm on the inner race measured at 1750 rpm and 2 hp

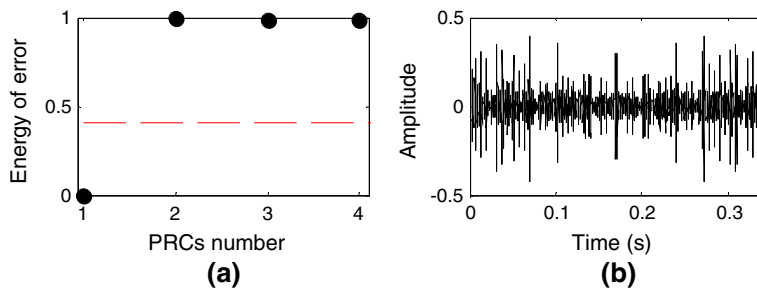


Fig. 26 **a** Energy of error, **b** Reconstructed signal of bearing with fault diameter of 0.018 mm on the outer race measured at 1797 rpm and 0 hp

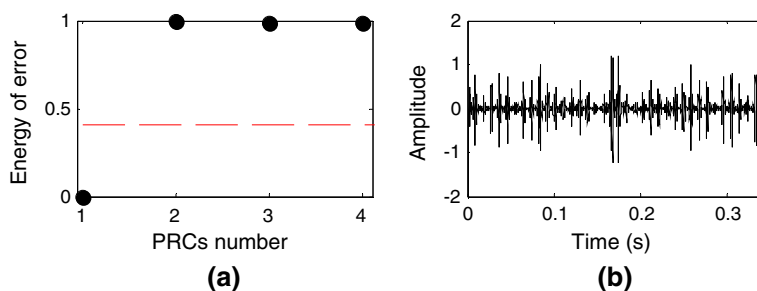


Fig. 27 **a** Energy of error, **b** Reconstructed signal of bearing with fault diameter of 0.018 mm on the outer race measured at 1750 rpm and 2 hp

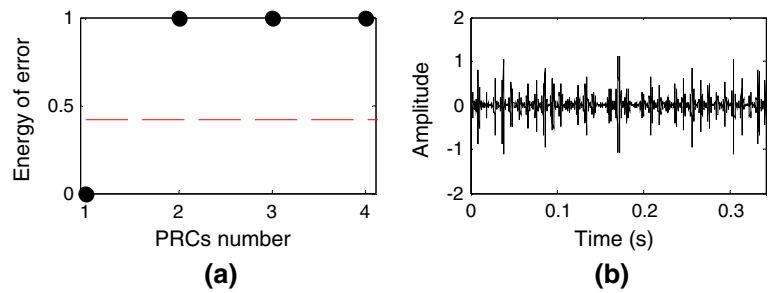


Fig. 28 **a** Energy of error, **b** Reconstructed signal of bearing with fault diameter of 0.053 mm on the inner race measured at 1797 and 0 hp

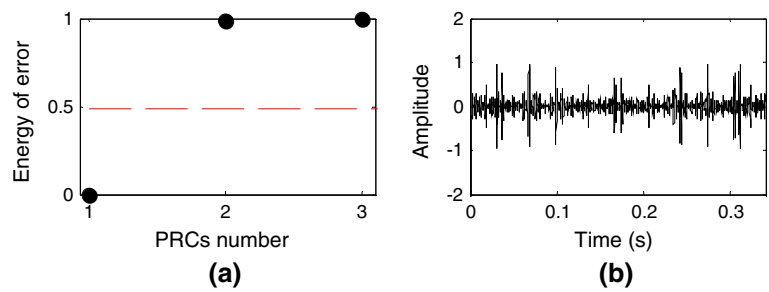


Fig. 29 **a** Energy of error, **b** Reconstructed signal of bearing with fault diameter of 0.053 mm on the inner race measured at 1750 rpm and 2 hp

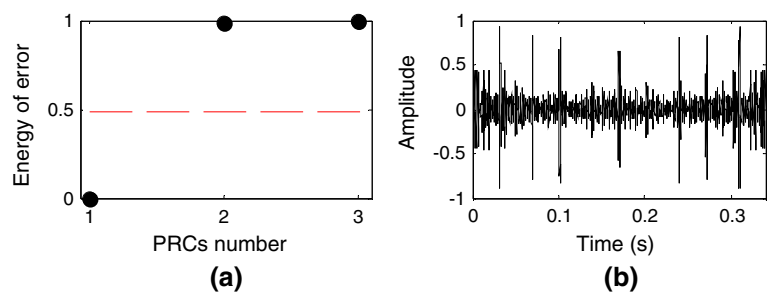


Fig. 30 **a** Energy of error, **b** Reconstructed signal of bearing with fault diameter of 0.053 mm on the outer race measured at 1797 rpm and 0 hp

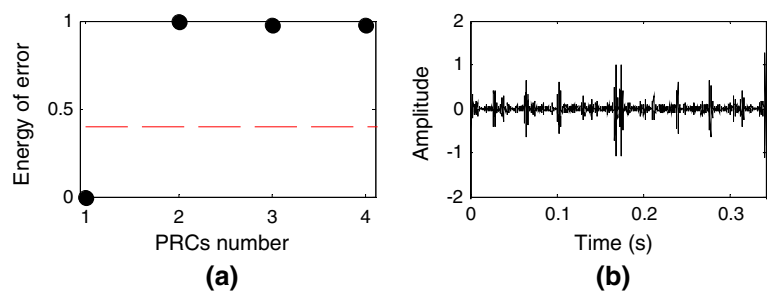


Fig. 31 **a** Energy of error, **b** Reconstructed signal of bearing with fault diameter of 0.053 mm on the outer race measured at 1750 rpm and 2 hp

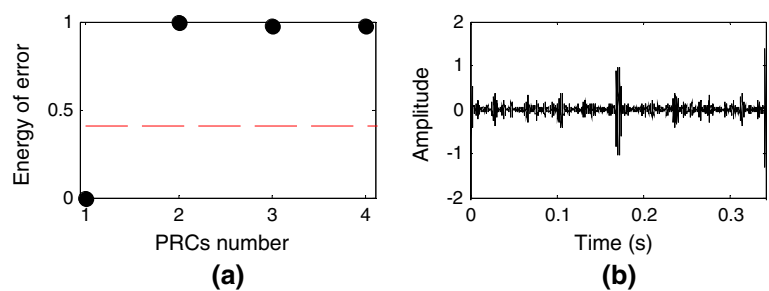


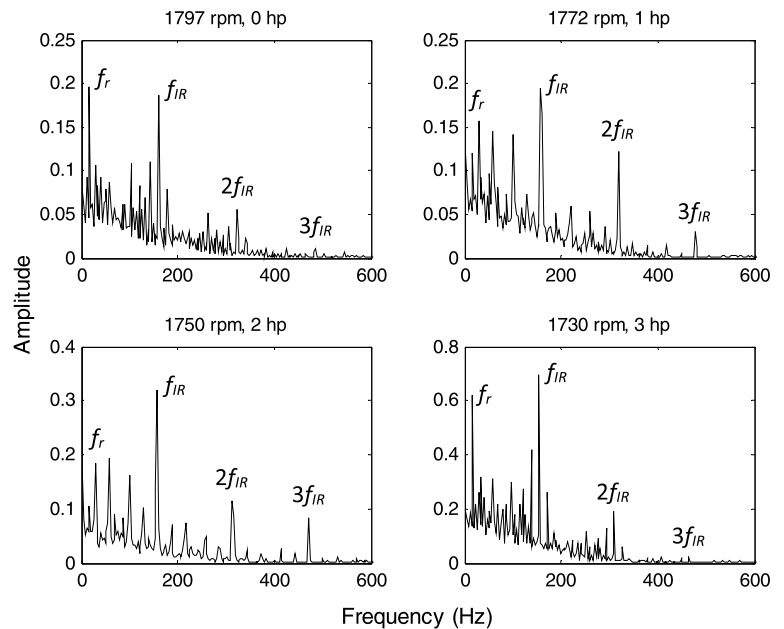
Table 3 σ and f_c of bearing with inner race fault

Fault diameter (mm.)	Rotation speed (rpm)	Load (hp)	σ (Hz)	f_c (Hz)
0.018	1797	0	2397	3483
	1772	1	2400	3451
	1750	2	2400	3438
	1730	3	2400	3393
0.053	1797	0	2400	2996
	1772	1	2400	2963
	1750	2	2400	2949
	1730	3	2400	2941

Table 4 σ and f_c of bearing with outer race fault

Fault diameter (mm.)	Rotation speed (rpm)	Load (hp)	σ (Hz)	f_c (Hz)
0.018	1797	0	2396	3619
	1772	1	2396	3592
	1750	2	2396	3558
	1730	3	2397	3598
0.053	1797	0	2396	3562
	1772	1	2396	3631
	1750	2	2397	3535
	1730	3	2398	3574

Fig. 32 Envelope power spectrum of the reconstructed signal of bearing with fault diameter of 0.018 mm on the inner race



5 Conclusion

This study presents a new time–frequency methodology, called CTFM, which combines the MWF, ITD, and TK operator to optimize the Morlet filter parameters and detect periodic impulses hidden in a vibration signal delivered from a rolling bearing. Firstly, the bearing vibration signal is filtered by MWF, with multiple values of σ and f_c , to reduce the noise component. In the second step, the resulting signal is decomposed into a number of PRCs by the ITD process

to eliminate interference components. Then, the significant PRCs are performed using the error measure criterion between the filtered signal and each mode of decomposition. By choosing the universal thresholding, a high value of this criterion indicates an insignificant PRC which must be eliminated before reconstruction. The main purpose of signal reconstruction is to extract the impulse components from the vibration signal. Finally, the TK operator is applied to demodulate the reconstructed signal and compute its energy via the proposed indicator. The optimal parameters of the

Fig. 33 Envelope power spectrum of the reconstructed signal of bearing with fault diameter of 0.053 mm on the inner race

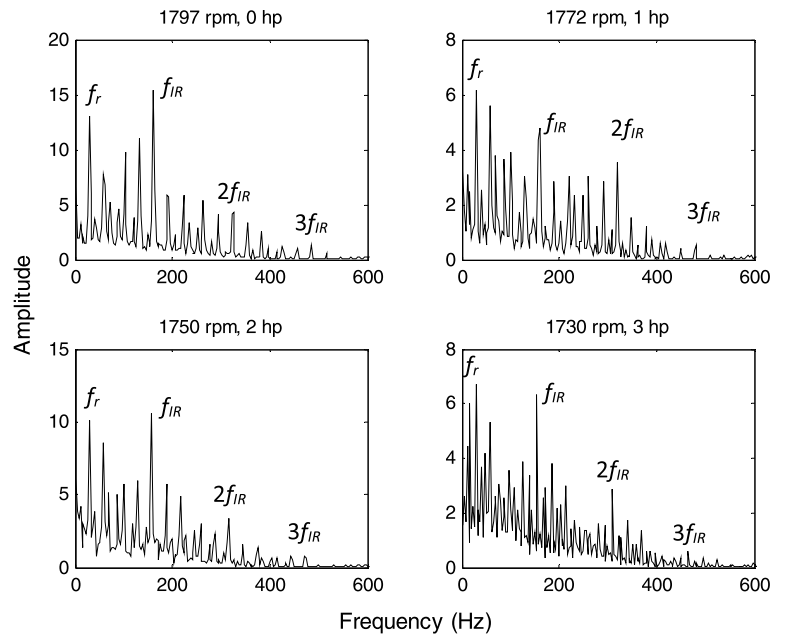


Fig. 34 Envelope power spectrum of the reconstructed signal of bearing with fault diameter of 0.018 mm on the outer race

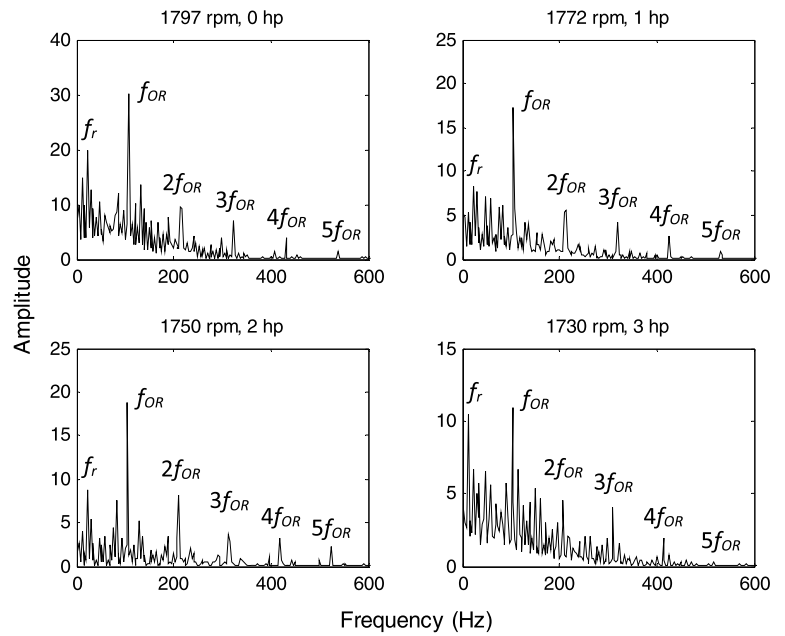


Fig. 35 Envelope power spectrum of the reconstructed signal of bearing with fault diameter of 0.053 mm on the outer race

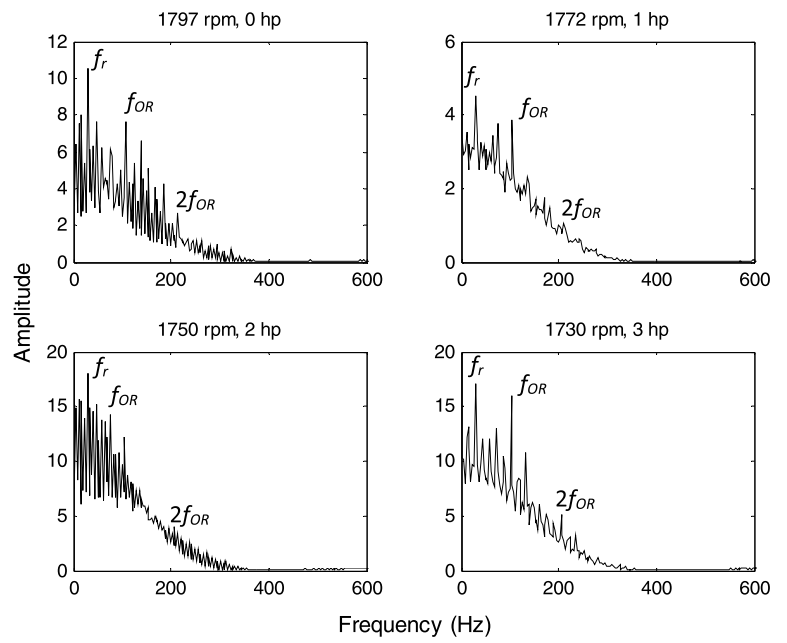


Fig. 36 Envelope power spectrum of the reconstructed signal of normal bearing

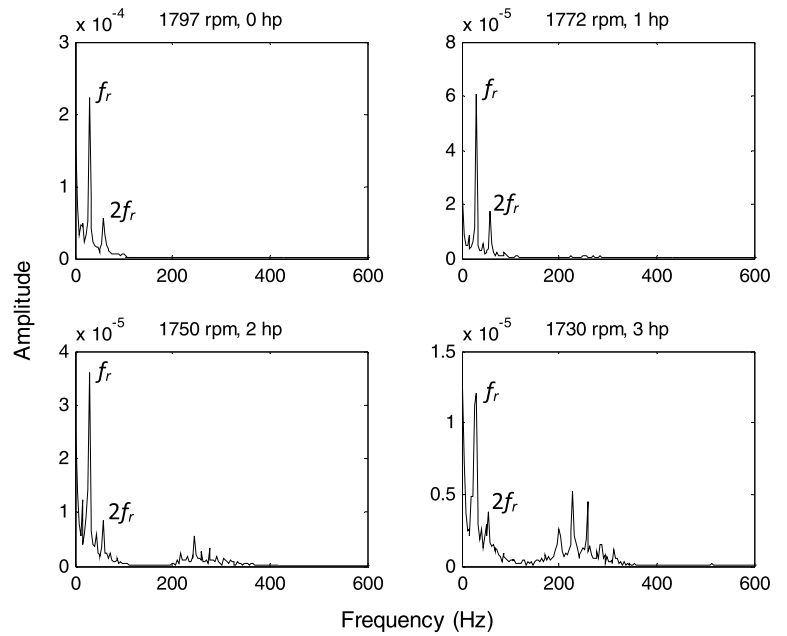


Table 5 Comparison between the proposed CTFM and the method of Su et al. [5]

Method	Su et al. [5] MWF + Genetic algorithm + Autocorrelation enhancement algorithm	Proposed method MWF + ITD + TK
Criterion	Shanon-entropy	Energy indicator (E_n)
NR Bearing		
f_c	1054	1200
σ	519	2400
Bearing with inner race fault		
f_c	2718	3451
σ	1359	2400
Bearing with outer race fault		
f_c	3498	3592
σ	1054	2396
f_r detection		
NR	f_r and its harmonic	f_r and its harmonic
IR	f_r and its harmonic	f_r and 2 harmonics
OR	f_r alone	f_r and 2 harmonics
BCFs detection		
IR	f_{IR} and its harmonic	f_{IR} and 2 harmonics + Sidebands
OR	f_{OR} and 2 harmonics	f_{OR} and 4 harmonics

Morlet filter are retained, according to the maximum energy value, and the corresponding envelope is transformed into a frequency spectrum to identify the BCFs.

The effectiveness of the proposed method is validated using a simulated vibration signal and experimental signals with different bearing conditions, different loads, several rotation speeds, and various sizes of faults. The obtained results show that the periodic impulses can be effectively extracted from the noisy input signals using the optimized MWF. Moreover, the frequency components corresponding to BCFs and their multiples are clearly identified in the envelope spectra. Therefore, it is obvious that CTFM is more suitable for extracting periodic impulses, generating optimal Morlet filters, and providing all BCFs. The proposed CTFM with operator's knowledge can improve the accuracy and efficiency of bearing condition monitoring.

References

1. Yu JB (2012) Local and nonlocal preserving projection for bearing defect classification and performance assessment. *IEEE Trans Industr Electron* 59(5):2363–2376. <https://doi.org/10.1109/TIE.2011.2167893>
2. Peng ZK, Chu FL (2004) Application of the wavelet transform in machine condition monitoring and fault diagnostics: a review with bibliography. *Mech Syst Sig Process* 18:199–221. [https://doi.org/10.1016/S0888-3270\(03\)00075-X](https://doi.org/10.1016/S0888-3270(03)00075-X)
3. Nikolaou NG, Antoniadis IA (2002) Demodulation of vibration signals generated by defects in rolling element bearings using complex shifted morlet wavelets. *Mech Syst Sig Process* 16(4):677–694. <https://doi.org/10.1006/mssp.2001.1459>
4. He W, Jiang ZN, Feng K (2009) Bearing fault detection based on optimal wavelet filter and sparse code shrinkage. *Measurement* 42:1092–1102. <https://doi.org/10.1016/j.measurement.2009.04.001>
5. Su W, Wang F, Zhu H, Zhang Z, Guo Z (2010) Rolling element bearing faults diagnosis based on optimal Morlet wavelet filter and autocorrelation enhancement. *Mech Syst Sig Process* 24:1458–1472. <https://doi.org/10.1016/j.ymssp.2009.11.011>
6. Jiang Y, Tang B, Qin Y, Liu W (2011) Feature extraction method of wind turbine based on adaptive Morlet wavelet and SVD. *Renewable Energy* 36:2146–2153. <https://doi.org/10.1016/j.renene.2011.01.009>
7. Zhang Y, Tang B, Liu Z, Chen R (2015) An adaptive demodulation approach for bearing fault detection based on adaptive wavelet filtering and spectral subtraction. *Meas Sci Technol* 27(2):025001. <https://doi.org/10.1088/0957-0233/27/2/025001>
8. Cao Y, Liu M, Yang J, Cao Y, Fu W (2018) A method for extracting weak impact signal in NPP based on adaptive Morlet wavelet transform and kurtosis. *Prog Nucl Energy* 105:211–220. <https://doi.org/10.1016/j.pnucene.2017.09.015>
9. Huang N, Shen Z, Long S et al (1998) The empirical mode decomposition and the Hilbert spectrum for nonlinear and non-stationary time series analysis. *Proc R Soc A Math Phys Eng Sci* 454:903–995. <https://doi.org/10.1098/rspa.1998.0193>
10. Smith JS (2005) The local mean decomposition and its application to EEG perception data. *J R Soc Interface* 2(5):443–454. <https://doi.org/10.1098/rsif.2005.0058>
11. Frei MG, Osorio I (2007) Intrinsic time-scale decomposition: Time–frequency–energy analysis and real-time filtering of non-stationary signals. *Proc Roy Soc London Ser A Math Phys Eng Sci* 463(2078):321–342. <https://doi.org/10.1098/rspa.2006.1761>
12. Zhang X, Zhang Q, Qin X, Sun Y (2016) Rolling bearing fault diagnosis based on ITD Lempel–Ziv complexity and PSO-SVM.

- J Vib Shock 35:102–107. <https://doi.org/10.13465/j.cnki.jvs.2016.24.017>
13. Yu J, Liu H (2018) Sparse Coding Shrinkage in Intrinsic Time-Scale Decomposition for Weak Fault Feature Extraction of Bearings. *IEEE Trans Instrum Meas* 67(7):1579–1592. <https://doi.org/10.1109/TIM.2018.2801040>
 14. Yu M, Pan X (2020) A novel ITD-GSP-based characteristic extraction method for compound faults of rolling bearing. *Measurement* 159:107736. <https://doi.org/10.1016/j.measurement.2020.107736>
 15. An X, Jiang D (2014) Bearing fault diagnosis of wind turbine based on intrinsic time-scale decomposition frequency spectrum. *Proc IMechE Part O: J Risk and Reliability* 228(6):558–566. <https://doi.org/10.1177/1748006X14539678>
 16. Sheng J, Dong S, Liu Z (2016) Bearing fault diagnosis based on intrinsic time-scale decomposition and improved Support vector machine model. *J Vibroengineering* 18(2):849–859
 17. Feng Z, Lin X, Zuo MJ (2016) Joint amplitude and frequency demodulation analysis based on intrinsic time-scale decomposition for planetary gearbox fault diagnosis. *Mech Syst Sig Process* 72:223–240. <https://doi.org/10.1016/j.ymsp.2015.11.024>
 18. Randall RB, Antoni J (2011) Rolling element bearing diagnostics – A tutorial. *Mech Syst Sig Process* 25(2):485–520. <https://doi.org/10.1016/j.ymsp.2010.07.017>
 19. Liang M, Soltani Bozchalooi I (2010) An energy operator approach to joint application of amplitude and frequency-demodulations for bearing fault detection. *Mech Syst Sig Process* 24:1473–1494. <https://doi.org/10.1016/j.ymsp.2009.12.007>
 20. Rodríguez PH, Alonso JB, Ferrer MA (2013) Travieso C.M., Application of the Teager-Kaiser energy operator in bearing fault diagnosis. *ISA Trans* 52:278–284. <https://doi.org/10.1016/j.isatra.2012.12.006>
 21. Ma J, Wu J, Wang X (2018) Incipient fault feature extraction of rolling bearings based on the MVMD and Teager energy operator. *ISA Trans* 80:297–311. <https://doi.org/10.1016/j.isatra.2018.05.017>
 22. Gu R, Chen J, Hong R, Wang H, Wu W (2020) Incipient fault diagnosis of rolling bearings based on adaptive variational mode decomposition and Teager energy operator. *Measurement* 149:106941. <https://doi.org/10.1016/j.measurement.2019.106941>
 23. Chui CK (2014) An introduction to wavelets, 1st edn. Academic Press
 24. Bendjama H, Boucherit MS (2016) Wavelets and principal component analysis method for vibration monitoring of rotating machinery. *J Theor Appl Mech* 54(2):659–670. <https://doi.org/10.15632/jtam-pl.54.2.659>
 25. Donoho DL, Johnstone IM (1994) Ideal spatial adaptive via wavelet shrinkage. *Biometrika* 81:425–455. <https://doi.org/10.2307/2337118>
 26. Kaiser JF (1990) On a simple algorithm to calculate the ‘energy’ of a signal. *Int Conf on Acoustics, Speech, and Signal Process.* 1:381–384. <https://doi.org/10.1109/ICASSP.1990.115702>
 27. Loparo KA (2003) Bearings vibration data set, Case Western Reserve University, (<http://www.eecs.cwru.edu>)
 28. Wang D, Guo W, Wang X (2013) A joint sparse wavelet coefficient extraction and adaptive noise reduction method in recovery of weak bearing fault features from a multi-component signal mixture. *Appl Soft Comput* 13:4097–4104. <https://doi.org/10.1016/j.asoc.2013.05.015>
 29. Gu X, Yang S, Liu Y, Deng F, Ren B (2018) Compound faults detection of the rolling element bearing based on the optimal complex Morlet wavelet filter. *J Mech Eng Sci* 232(10):1786–1801. <https://doi.org/10.1177/0954406217710673>
 30. Albezzawy MN, Nassef MG, Sawalhi N (2020) Rolling element bearing fault identification using a novel three-step adaptive and automated filtration scheme based on Gini index. *ISA Trans* 101:453–460. <https://doi.org/10.1016/j.isatra.2020.01.019>

Publisher's Note Springer Nature remains neutral with regard to jurisdictional claims in published maps and institutional affiliations.

Springer Nature or its licensor holds exclusive rights to this article under a publishing agreement with the author(s) or other rightsholder(s); author self-archiving of the accepted manuscript version of this article is solely governed by the terms of such publishing agreement and applicable law.